DIURNAL DYNAMICS OF EVAPOTRANSPIRATION AND SURFACE ENERGY BUDGET IN GIANT JUNCAO *(CENCHRUS FUNGIGRAMINUS)* UNDER SUMMER WEATHER VARIABILITY

WANG, Z. Y.[1#] – LI, S. F.[1#] – LV, S.[2] – YAN, H. H.[2] – LIN, Z. X.[2] – LIN, D. M.[2*] – LIU, F. S.[2*]

[1]*College of Forestry, Fujian Agriculture and Forestry University, Fuzhou Fujian 350007, China*

[2]*College of JunCao Science and Ecology (College of Carbon Neutrality) /China National Engineering Research Center of JUNCAO Technology, Fuzhou Fujian 350007, China*

[#]*These authors contributed equally.*

[*]*Corresponding authors*
e-mail: wzy201897@sina.com; Liufengshan0225@163.com; phone: +86-188-5914-8751

(Received 19th Sep 2024; accepted 24th Jan 2025)

Abstract. The examination of the dynamic characteristics of water vapor and energy exchange under the backdrop of global climate change is crucial for the sustainable utilization and management of water resources, particularly in agricultural regions where water is a scarce commodity. Based on the water and heat flux data and meteorological information collected by the Bowen ratio flux column of the Giant Juncao *(Cenchrus fungigraminus)* ecosystem in the semi-arid region of northwest China in 2022, the energy balance method and plate heat flux method were used to calculate the energy exchange and evapotranspiration indicators, and the changes of energy balance and evapotranspiration under different weather conditions were explored. The influence of Giant Juncao *(Cenchrus fungigraminus)* on surface energy balance; The main driving factors of evapotranspiration and Bowen ratio change. The findings show that solar radiation during summer weather exhibits a single-peak pattern, with peak intensity ranked as clear > cloudy > rainy days. Net radiation follows a single-peak trajectory on clear days, varies significantly on cloudy days, and forms a 'concave' pattern on rainy days. The mean net radiation is highest on cloudy days, followed by rainy and then clear days. Specifically, cloudy days register 527.41 W/m^2 more net radiation than clear days and 343.28 W/m^2 more than rainy days every 10 minutes. Surface reflected radiation, under all weather scenarios, adheres to a single-peak pattern. There is a positive correlation between solar radiation, temperature, and surface reflectance, with the presence of Giant Juncao enhancing reflectance. The average annual surface reflectance of the Giant Juncao ecosystem is 0.28, with the following order: clear days < cloudy days < rainy days. Latent heat flux manifests a single-peak pattern on clear days, a wave-like trend on cloudy days, and its magnitude on rainy days is contingent upon rainfall timing, showing reduced latent heat flux during rainfall and an increase in the atmosphere's latent heat flux during dry spells. The diurnal range of sensible heat flux is greatest on clear days, followed by cloudy and rainy days, mirroring the pattern observed in soil heat flux. Both the Bowen ratio and evapotranspiration exhibit a single-peak variation across all weather conditions. Evapotranspiration totals 0.74 mm on clear days, which is lower than the 1.41 mm observed on cloudy days but higher than the 0.45 mm on rainy days. The average Bowen ratio across different weather conditions follows the sequence: cloudy days > clear days > rainy days. Solar radiation emerges as the principal driver of evapotranspiration and the Bowen ratio, with additional influences from air temperature, wind speed, and soil moisture content under varying weather conditions. This study of energy partitioning within the Giant Juncao ecosystem under diverse weather scenarios lays the groundwork for future propagation and cultivation of Giant Juncao in the equatorial zone and the semi-arid regions of Northwest China.
Keywords: *different weather, energy change, evapotranspiration, Bowen ratio*

Introduction

In Earth's atmospheric system, the transfer and transformation of energy are pivotal for sustaining the climate equilibrium. Solar radiation, the principal energy source for the

http://www.aloki.hu ● ISSN 1589 1623 (Print) ● ISSN1785 0037 (Online)
DOI: http://dx.doi.org/10.15666/aeer/2304_65756595

Earth's surface, is absorbed and re-emitted by the atmosphere as sensible heat flux, subsequently being transmitted to the ground. Terrestrial vegetation drives evapotranspiration (ET), transferring water from plant surfaces and soil to the atmosphere as latent heat flux, a key component of energy exchange (Zhou and Huang, 2014). Atmospheric energy is primarily conveyed through sensible and latent heat fluxes. Sensible heat flux denotes the direct heat transfer between the atmosphere and the Earth's surface, driven by temperature gradients and manifesting as temperature fluctuations (Zhou and Huang, 2010). Conversely, latent heat flux pertains to the heat that is either liberated or absorbed during phase transitions (Banerjee, 2013). Predominantly, latent heat flux in nature is associated with the phase changes of water, and it is thus characterized in the realms of atmospheric and remote sensing sciences as the thermal interchange of water between the underlying surface and the atmosphere, predominantly via plant transpiration and precipitation. Rainfall is a crucial component of the water cycle, redistributing latent heat from the atmosphere to the Earth's surface. The release of this latent heat subsequently influences the surface energy balance. Latent heat flux is synonymous with evapotranspiration, which encompasses not only plant transpiration but also the evaporation of moisture from soil and plant surfaces. During evaporation, a significant amount of heat is absorbed, leading to a reduction in surface temperatures and the return of energy to the atmosphere in the form of latent heat. This exchange of energy regulates the surface-atmosphere balance and influences local climate (Yang et al., 2023). The surface energy balance is characterized by the dynamic equilibrium between the solar radiation absorbed by the Earth's surface, the long-wave radiation emitted into the atmosphere and back to the ground, and the energy conveyed to the atmosphere via sensible and latent heat exchanges. Shifts in this equilibrium state are intricately linked to critical climatic variables such as surface temperature, humidity, and atmospheric circulation, particularly within non-humid region ecosystems (Wang and Li, 2011). Consequently, investigating the dynamics of surface energy balance and evapotranspiration in arid regions, their environmental responses, and the prevailing factors under diverse weather conditions, is of paramount importance. Such inquiries are essential for comprehending the global climate system, forecasting water resource tendencies, devising prudent water resource management strategies, and evaluating the resilience of ecosystems.

Semi-arid regions constitute a substantial 40% of the Earth's land surface and are recognized as some of the most sensitive and delicate ecosystems globally (Smith et al., 2019; Ullah et al., 2022). The northwestern region of China, characterized by its quintessential semi-arid agricultural landscapes, underscores the importance of sustainable agricultural development (Hu et al., 2022). Research in this area, particularly focusing on the judicious management of water resources and the conservation of the ecological environment, is crucial for bolstering agricultural productivity and enhancing crop quality. The cultivation of Giant Juncao (*Cenchrus fungigraminus*) presents a multifaceted solution for semi-arid agricultural zones. It plays a pivotal role in combating soil erosion, alleviating the detrimental effects of soil salinization, and doubling as a substrate for the cultivation of edible fungi. Additionally, it serves as a biomass energy source, contributing to the diversification of agricultural outputs and augmenting the efficiency of the livestock sector. These benefits are instrumental in stimulating the local economy (Liu et al., 2010). Consequently, a thorough investigation into the evapotranspiration (ET) and energy transformation processes within the Giant Juncao ecosystem is warranted. Such research is essential for gaining insights into the ecological

http://www.aloki.hu ● ISSN 1589 1623 (Print) ● ISSN1785 0037 (Online)
DOI: http://dx.doi.org/10.15666/aeer/2304_65756595

and economic potential of this versatile plant in semi-arid regions, informing strategies for sustainable land management, and optimizing agricultural practices for the future.

Giant Juncao *(Cenchrus fungigraminus)*, an upright tufted plant of the monocotyledonous grass family of the genus pennisetum. Originally, from KwaZulu-Natal Province in South Africa, it was meticulously introduced to China in 2006 by the Edible Fungi Research Institute at Fujian Agriculture and Forestry University for cultivation (Lin et al., 2014). This versatile plant thrives in tropical, subtropical, and temperate climates, earning its reputation as a high-yield, superior quality forage (Li et al., 2019). Distinctive for its towering stature and clumped architecture, Giant Juncao boasts an extensive root system that permits vigorous growth even in the deepest soil strata. Beyond its role as premium fodder, it confers a trove of ecological, economic, and societal advantages (Song et al., 2023). Ecologically, Giant Juncao emerges as a vanguard in the battle against desertification. Its swift growth cycle and profound root network ensure swift, impactful, and enduring outcomes in windbreak and sand stabilization efforts (Sheng, 2023). Consequently, it has become an indispensable asset in soil and water conservation initiatives, as well as in broader environmental management strategies focused on windbreak and sand fixation.

With the widespread adoption of Giant Juncao (*Cenchrus fungigraminus*) in China's northwestern regions, understanding its evapotranspiration across diverse weather scenarios is crucial for deciphering the energy dynamics and fluxes within this ecosystem. This research draws upon meteorological and energy data, collected by the Bowen ratio flux tower located at the Hongsheng Juncao Technology Innovation Industrial Park in Baofeng Town, Pingluo County, Shizuishan City, Ningxia. It offers a comprehensive analysis of the surface energy balance components within the Giant Juncao ecosystem of the semi-arid northwestern Chinese agricultural fields under three distinct meteorological conditions: clear, cloudy, and rainy days. The study aims to unravel the characteristics and determinants of the surface energy balance and its partitioning within the Giant Juncao ecosystem under varying weather patterns. This finding is crucial to deepen our understanding of the water budget, land use and inherent energy cycle processes of the Giant Juncao ecosystem in semi-arid regions, and will help provide technical support and scientific guidance for the subsequent spread of Giant Juncao in semi-arid regions and equatorial regions to provide reasonable irrigation management measures. Ultimately, it will help develop smarter ecological and agricultural strategies in these areas.

Materials and methods

Overview of the study area

Nestled within the Hongsheng Juncao Technology Innovation Industrial Park in Baofeng Town, Pingluo County, Shizuishan City, Ningxia (coordinates 39°4′48.36″N, 106°43′27.96″E, and an elevation of 1,068 meters), *Figure1*, the experimental site boasts a flat topography, with the Helan Mountain Range serving as a backdrop to the northwest. Characterized by a temperate continental semi-arid climate, this region enjoys an average annual temperature of 10.8°C, receives a modest annual precipitation of 191.7 mm, and maintains an average annual relative humidity of 44.4%. The soil, classified as loamy, is quintessential for the area (Liu et al., 2023). The experimental site undergoes a cycle of pronounced seasonal changes: a spring that is dry and windy, yet experiences a swift ascent in temperatures; a summer that is hot and sees rainfall in intense bursts; an autumn that is fleeting and marked by a rapid descent in temperatures; and a winter that is cold,

http://www.aloki.hu ● ISSN 1589 1623 (Print) ● ISSN1785 0037 (Online)
DOI: http://dx.doi.org/10.15666/aeer/2304_65756595

with infrequent snow and rain, the majority of precipitation occurring from June through October (Xu et al., 2013). The cultivation of Giant Juncao commences on May 1st and extends to October 15th. This plant is propagated in a row pattern through the use of rhizomes, achieving an average height of 4.15 meters during the cultivation period. The planting scheme adheres to a grid, with a square spacing of 0.6 meters by 0.6 meters, ensuring optimal growth and development (Liu et al., 2023).

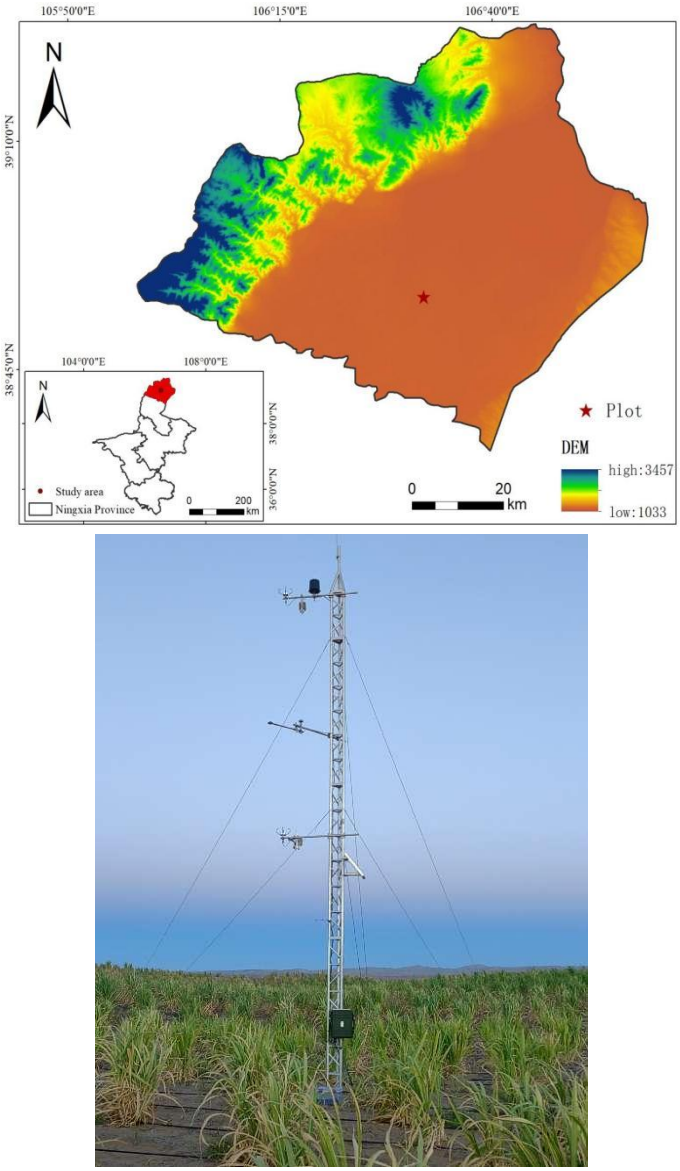

Figure 1. *Study area location and test site Bowen ratio flux tower*

Change characteristics of environmental factors during the experiment

Throughout the experimental phase, spanning July 1 to August 30, meteorological parameters were meticulously documented as depicted in *Figure 2*. The saturation vapor pressure deficit and ambient air temperature exhibited a relative stability, contrasted by the erratic distribution of rainfall. The thermal amplitude was marked by a peak air temperature of 40.89°C and a nadir of 17.25°C, culminating in a mean temperature of

http://www.aloki.hu ● ISSN 1589 1623 (Print) ● ISSN1785 0037 (Online)
DOI: http://dx.doi.org/10.15666/aeer/2304_65756595

25.4°C. The saturation vapor pressure deficit oscillated within the range of 0.5 to 2.0 kPa, with a discernible downward trend in August, concurrent with a general ascent in air temperature. The cumulative rainfall for the experimental duration was 68mm, constituting 31.48% of the annual precipitation total. Notably, the zenith of rainfall events was registered on July 11 and August 13, amassing 13.2mm and 13.4mm respectively. These precipitation peaks corresponded with pronounced variations in the saturation vapor pressure deficit, indicative of the direct influence of rainfall on this parameter, which is also subject to temperature fluctuations.

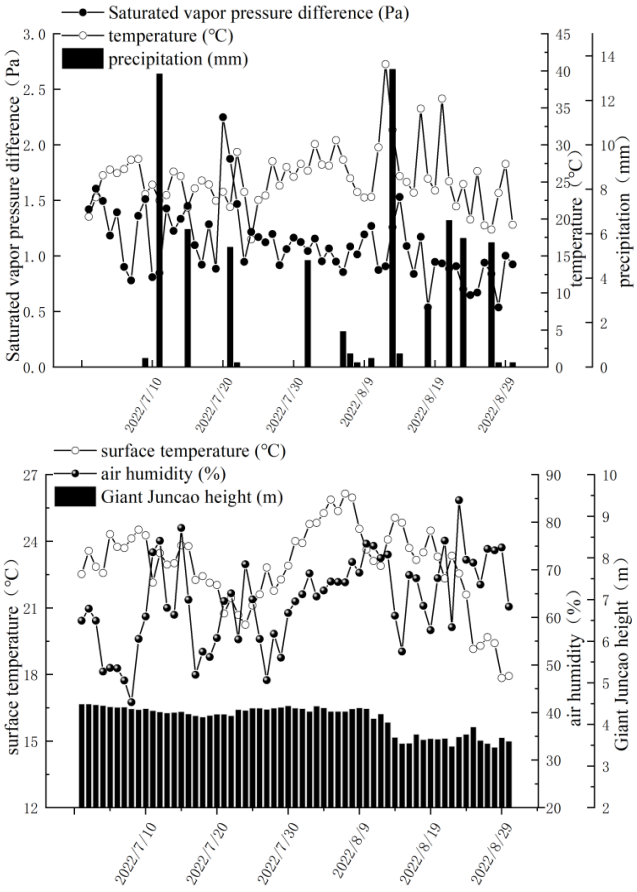

Figure 2. *Meteorological factors during the test*

The Giant Juncao vegetation, under experimental scrutiny, maintained an average stature of 4.14 meters. In the experiment's waning days, the vegetation was modestly impacted by elevated wind velocities, leading to slight lodging and a subsequent reduction in overall height. The atmospheric humidity demonstrated a dynamic range, oscillating between 40% and 90%. The acme of humidity, reaching 84.64%, was observed on August 23 during a rainy episode, whereas the nadir, at 46.81%, coincided with an air temperature apex on July 27. The experiment's average atmospheric humidity settled at 54.88%, surpassing the annual average of less than 35% recorded in the arid Alxa Desert yet falling short of the approximately 70% humidity typical of China's humid regions (Li et al., 2022; Wang et al., 2024). Akin patterns of increase were noted for both surface temperature and atmospheric humidity from late July to early August, driven by the escalating air temperatures. Conversely, as the experiment progressed into the latter half,

http://www.aloki.hu ● ISSN 1589 1623 (Print) ● ISSN1785 0037 (Online)
DOI: http://dx.doi.org/10.15666/aeer/2304_65756595

a decline in air temperatures post mid-August precipitated a gradual reduction in surface temperature. Over the experimental tenure, surface temperatures wavered within the band of 18 to 27°C.

Data source and processing

The experimental dataset spans the period from July 1 to August 30, 2022, and was procured through the deployment of a Bowen ratio energy flux tower, which was utilized to assess both energy and meteorological parameters. The specifications of the Bowen ratio energy flux tower are delineated in the *Table 1*. The data collection was executed at 10-minute intervals, capturing a spectrum of meteorological variables including temperature, humidity, actual vapor pressure, and precipitation, alongside energy fluxes such as latent heat flux, sensible heat flux, and soil heat flux. Throughout the experimental timeframe, a total of 18 precipitation events were recorded, with 7 days registering a mean precipitation exceeding 5 mm, signifying a typical rainfall pattern for the experimental locale. For the purposes of this analysis, distinct meteorological conditions were isolated: typical clear days (July 20 and August 16), cloudy days (July 2 and August 26), and rainy days (July 11 and August 23). The nocturnal period was demarcated from 19:00 to 07:00, with the diurnal period extending from 07:00 to 19:00. The selection of cloudy days was predicated on the days immediately before and after precipitation events, with additional criteria informed by manual observations and shifts in meteorological indicators, such as the relatively lower atmospheric pressure, attenuated solar radiation, and reduced diurnal temperature variation characteristic of cloudy conditions (Li et al., 2012). Visualization of the data was facilitated through the application of Origin2021 software, while data manipulation and preparation were conducted employing Excel2010. Subsequent data analysis was performed using the SPSS software suite, ensuring a robust and methodologically sound approach to interpreting the collected dataset.

Table 1. *Instrument overview of Bowen ratio flux tower*

Name	Type	Precision
Air temperature and humidity sensor	RR14TH	Temperature accuracy ±0.1°C, humidity accuracy ±1%; Installation height: 5, 10
Two-dimensional ultrasonic wind speed sensor	RR20WU	Wind speed measurement accuracy ±2%; Wind speed resolution 0.01 m·s^-1; Wind direction measurement range 0° to 359° without dead zone; Wind direction accuracy ±3°; Wind direction resolution 1°; Installation height: 5, 10 m
Solar radiation sensor	RR20P	Range 0 to 2000 W·m^-2, accuracy ±5%, response spectrum 400 to 1100 nm; Installation height: 7 m, one downward and one upward
Net radiation sensor	RR71NR	Response spectrum 250 to 60000 nm; Calibration coefficient 9.6 to 11.9 W·m^-2·mV^-1; Installation height: 7 m
Barometric pressure sensor	RR410BP	Range 60,000 to 110,000 Pa; Accuracy ±100 Pa; Resolution 10 Pa; Installation height: 2 m
Ultrasonic distance sensors	SR50A	Measurement range 0.5 to 10 m; Accuracy ±1.0 cm or ±0.4% of target distance; Resolution 0.25 mm; Reception angle 30°; Measurement time <1.0 s; Installation height: 5 m
Rain sensor	RR3665R	Range 0 to 700 mm·h^-1; Accuracy ±2%; Resolution 0.2 mm; Installation height: 10 m
Soil heat flux sensor	RRHFT3	Range ±1000 W·m^-2; Accuracy ±5%; Sensitivity 50 μV·W^-2·m^-1; Installation depth: 5 cm, one in the east-west direction each
Soil moisture temperature sensor	RRECT5	Temperature: Range -40 to 65°C, accuracy ±0.2°C; Humidity: Range 0 to 100%, accuracy ±3%, resolution 0.1%; Installation depth: 2, 4, 10, 20, 40 cm

http://www.aloki.hu ● ISSN 1589 1623 (Print) ● ISSN1785 0037 (Online)
DOI: http://dx.doi.org/10.15666/aeer/2304_65756595

Calculation method of each index

In this study, evapotranspiration is quantified using data procured from the Bowen ratio energy flux tower. The Bowen ratio energy balance approach is anchored in the Bowen ratio and the fundamental energy balance equation, which asserts that the total energy flux absorbed by the Earth's surface is equivalent to the aggregate energy allocated for warming the air, vaporizing water, and facilitating other transformative energy processes (Bowen, 1926). A plethora of research has substantiated the efficacy and remarkable precision of this technique in assessing evapotranspiration rates (Zhang et al., 2019).

$$Rn = LE + H + G \quad \text{(Eq.1)}$$

In the equation, R_n represents the net radiation flux (W/m^2), LE denotes the latent heat flux (W/m^2), H signifies the sensible heat flux (W/m^2), and G indicates the soil heat flux (W/m^2).

The calculation formula for evapotranspiration (E) is as follows, where L represents the latent heat of vaporization of water, taken as 2500 kJ/kg:

$$E = \frac{R-G}{L(1+b)} \quad \text{(Eq.2)}$$

The calculation of surface soil heat flux employs the plate heat flux method, which involves calculating the surface soil heat flux by summing the observed heat flux at 5 cm depth with the heat storage of the soil above it. The calculation formula is as follows:

$$G = \mathrm{Ss} + G_{\mathrm{z}} \quad \text{(Eq.3)}$$

In the formula, G_z represents the measured value by the soil heat flux plate (W/m^2), S_s is soil heat accumulation.

Soil thermal energy storage refers to the energy within a certain depth below the soil surface and is expressed as:

$$S_s = C_s \frac{\Delta T_s}{\Delta t}\mathrm{z} \quad \text{(Eq.4)}$$

$$C_s = 0.85\rho_b + 4.2\theta_v \quad \text{(Eq.5)}$$

In the above equation, Cs is the soil specific heat capacity (J/kg·K), ΔT_s is the difference in soil temperature (K) measured at two adjacent time points, Δt is the time difference (s) between two adjacent measurements, z is the thickness of the soil layer (m) from the ground surface to the soil heat flux plate, ρ_b is the bulk density of the soil (g/cm^3), and θ_v is the soil volumetric water content (%).

The calculation formula for surface albedo (α) is as follows (Nie et al., 2019):

$$\alpha = R_{Sup}/R_{Sdown} \quad \text{(Eq.6)}$$

In the formula: R_{Sup} and R_{Sdown} represent the upward and downward shortwave radiation, respectively.

http://www.aloki.hu ● ISSN 1589 1623 (Print) ● ISSN1785 0037 (Online)
DOI: http://dx.doi.org/10.15666/aeer/2304_65756595

Result and analysis

Surface radiation characteristics of the Giant Juncao ecosystem

The *Figure 3* representations elucidate the distinct radiation variability traits of the Giant Juncao ecosystem across quintessential clear, cloudy, and rainy conditions. During periods of clear skies, solar and reflected surface radiations adhere to a pronounced unimodal pattern, while net radiation traces an initial upward trajectory, culminating in a gradual decline, punctuated by minor oscillations. These manifestations mirror the radiative fluctuations within the oasis-desert transitional zones during cloudless days (Li et al., 2012). Characterized by a well-delineated diurnal rhythm of surface radiative equilibrium, solar radiation on clear days exhibits a smooth and consistent progression. Influenced predominantly by atmospheric clarity and cloud cover, with the solar elevation angle exerting a comparatively negligible impact at a given observation site, the atmosphere, under cloudless conditions, presents heightened transparency and an absence of clouds (Li et al., 2012). Consequently, solar radiation peaks at 908 W/m^2, typically at noon (circa 13:00), coinciding with the zenith of solar intensity and the daily temperature apex. Post-14:00, the solar radiation commences its decline earlier than on cloudy and rainy days, attributable to the lack of clouds that would otherwise reflect solar radiation back to the earth's surface, thereby retarding the radiation's descent. On average, clear days witness solar radiation values of 311.41 W/m^2.

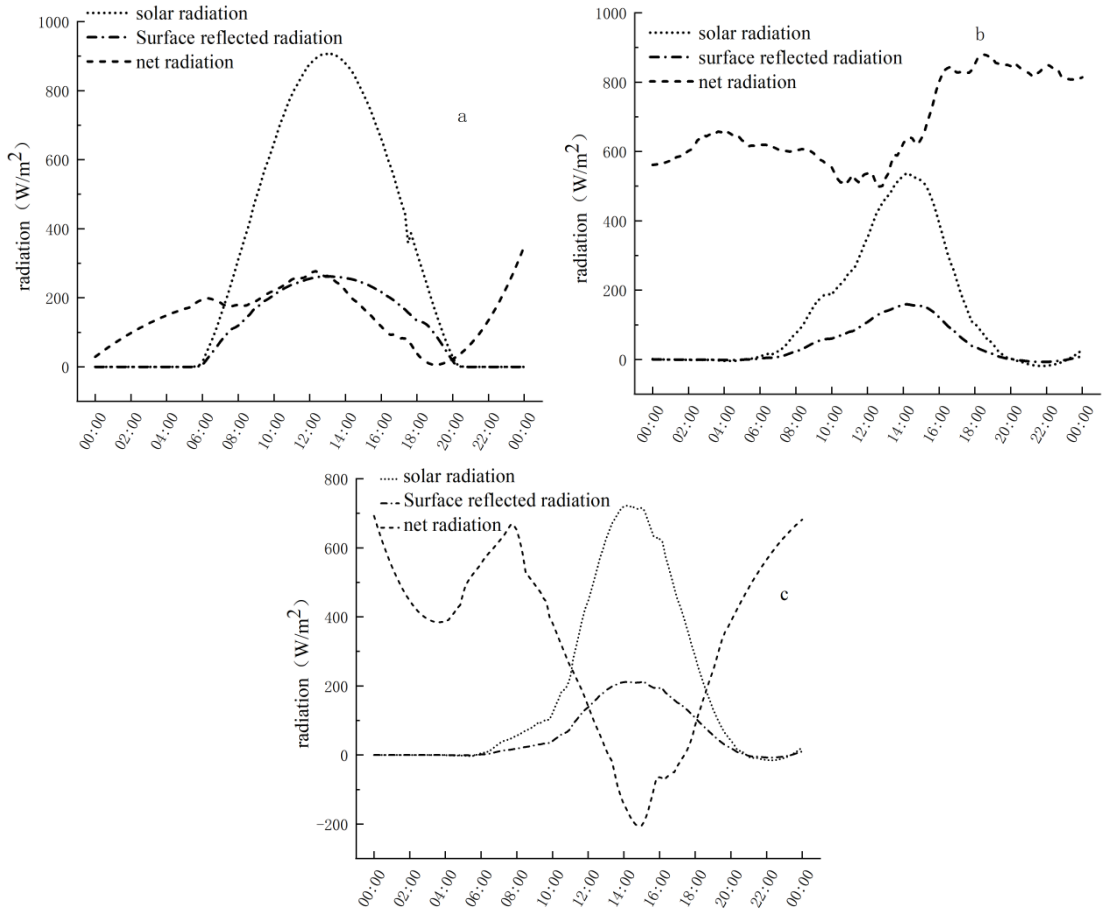

Figure 3. *Changes of solar radiation, surface reflected radiation and net radiation under sunny (a), cloudy (b) and rainy (c) days*

http://www.aloki.hu ● ISSN 1589 1623 (Print) ● ISSN1785 0037 (Online)
DOI: http://dx.doi.org/10.15666/aeer/2304_65756595

In stark contrast, cloudy conditions engender substantial variability in solar radiation intensity, a consequence of the incessant cloud dynamics. The zenith of solar radiation on cloudy days, reaching 870 W/m^2, is modestly diminished relative to clear days and emerges slightly later (around 14:00). Throughout the daylight hours, the intensity of solar radiation undergoes several fluctuations, a direct result of cloud obstruction and transformation (Xia et al., 2023). Nonetheless, the mean solar radiation on cloudy days stands at a considerably lower 137.14 W/m^2, a figure substantially below that of clear days.

On rainy days, solar radiation is most profoundly curtailed. The maximum solar radiation on such days, a mere 721.81 W/m^2, is not only significantly reduced from clear days but also from cloudy conditions. With an average value of 188.69 W/m^2, it underscores the minimal contribution of solar radiation to the ecosystem's energy budget during rainy periods.

In aggregate, the radiation variation characteristics of the Giant Juncao ecosystem are markedly dissimilar across diverse meteorological settings, with these disparities being instrumental for deciphering the ecosystem's surface energy balance and the underpinning ecological processes.

The maximum surface reflected radiation intensities are recorded at 262 W/m^2 on clear days, 79.45 W/m^2 on cloudy days, and 280.7 W/m^2 on rainy days. Relative to clear and rainy days, cloudy days exhibit the lowest surface reflected radiation, markedly less than both clear and rainy conditions. Conversely, rainy days are characterized by the highest surface reflected radiation. Contrary to these observations, the surface albedo of the Giant Juncao field, calculated across varying weather conditions, remains consistently around 0.3. This suggests that the surface albedo is minimally influenced by solar radiation due to the extensive coverage provided by the Giant Juncao, maintaining a relatively stable state with diffuse reflection being the predominant mode of solar radiation interaction during this period.

As detailed in the subsequent *Table 1*, the surface albedo of the Giant Juncao field surpasses the annual mean, particularly during the summer experimental phase, indicating that heightened solar radiation and temperatures are conducive to an increase in surface albedo. The soil moisture content, which is 34.79% in August compared to 35.21% in July, follows an overall declining trend, leading to a corresponding decrease in soil albedo from July (0.306) to August (0.291). This finding aligns with the research of Xiao Dengpan and colleagues (Li et al., 2018). The soil albedo, observed under diverse weather conditions throughout the experimental period, exceeds the annual average, underscoring the more pronounced impact of temperature on soil albedo in comparison to other factors.

In comparison to the Giant Juncao field, the surface albedo of bare soil is generally lower, with a gradient of clear days > cloudy days > rainy days, demonstrating that solar radiation and temperature are instrumental in augmenting surface albedo. Moreover, the contribution of Giant Juncao to the enhancement of surface albedo is substantial and warrants significant consideration.

Net radiation within the Giant Juncao ecosystem experiences significant fluctuations under different weather conditions. On clear days, net radiation starts with an upward trend, then declines, peaking at 442 W/m^2, with an average of 150.89 W/m^2 and a daily variation of 760.7 W/m^2. Cloudy days, on the other hand, are marked by a maximum net radiation of 955 W/m^2, a daily average of 678.3 W/m^2, and a diurnal fluctuation of 587.5 W/m^2. Rainy days show a maximum net radiation of 692.49 W/m^2, a daily average of 335.02 W/m^2, and a diurnal range of 898.12 W/m^2. The ranking of

http://www.aloki.hu ● ISSN 1589 1623 (Print) ● ISSN1785 0037 (Online)
DOI: http://dx.doi.org/10.15666/aeer/2304_65756595

maximum net radiation is cloudy days > rainy days > clear days, while the order of the diurnal range of net radiation is clear days > cloudy days > rainy days.

During overcast and rainy conditions, the net radiation is comparatively higher due to the increased atmospheric longwave radiation, surpassing that observed on clear days. On clear days, the interference from clouds and other meteorological elements is minimal, allowing for greater solar radiation to reach the ground and a reduced level of reflected radiation, thus amplifying the diurnal range of net radiation. Conversely, on cloudy and rainy days, the presence of clouds and raindrops attenuates solar radiation, and these meteorological phenomena reflect a portion of the solar radiation back into the atmosphere. Consequently, the solar radiation that penetrates to the ground is diminished, and the reflected component is enhanced, leading to a more subdued diurnal range of net radiation.

Surface energy characteristics of Giant Juncao Ecosystem

The energy flux dynamics within the Giant Juncao ecosystem under different weather conditions are depicted in *Figure 4*. On clear days, the latent heat flux follows a distinct unimodal curve, reaching its peak at 13:00 under the influence of the most intense solar radiation at noon. This peak solar radiation enhances the exchange of water vapor between the atmosphere and the ground, intensifying the evaporation process, with the flux reaching a maximum of 284.24 W/m^2. On cloudy days, the latent heat flux initially declines, hitting a low point at 10:00 with a value of 75.12 W/m^2, at the same time that the sensible heat flux reaches its peak at 305.6 W/m^2. Subsequently, the latent heat flux increases, reaching its daily high of 768.44 W/m^2 at 17:00. The latent heat flux on cloudy days exhibits a wave-like pattern, with peaks occurring between 3:00-5:00 and 17:00, the latter being more significant. At night, energy is predominantly expressed as latent heat, with the transition from day to night at 17:00 characterized by minimal surface radiation and a decrease in ground temperature, conditions that are conducive to water evaporation and the release of latent heat.

On rainy days, the latent heat flux adheres to a unimodal trajectory, maintaining a relatively stable level within a certain range for an extended period. The magnitude of the latent heat flux on rainy days is likely linked to the timing of rainfall; during rain events, the latent heat flux diminishes as atmospheric moisture is predominantly rain-derived. Throughout the rainfall, atmospheric water vapor condenses, releasing latent heat that accompanies the rain to the ground, rather than contributing directly to the atmospheric-surface latent heat flux. In the interstitial periods of rainfall, variations in atmospheric humidity prompt an uptick in latent heat flux. Post-rainfall, the augmentation of surface moisture and the resumption of solar radiation can intensify the evaporation process, consequently elevating the latent heat flux. Across the three weather scenarios, the maximum values and diurnal variations of the latent heat flux are ordered as rainy days > cloudy days > clear days.

The sensible heat flux, across various weather conditions, follows a unimodal pattern, with the magnitude of fluctuations being less pronounced on clear and rainy days compared to cloudy days. On clear days, the increased solar radiation leads to a rise in surface temperature as the ground absorbs this energy, creating a significant thermal gradient with the atmosphere. This gradient drives the transfer of sensible heat flux. In contrast, cloudy days are characterized by reduced atmospheric stability, with increased atmospheric turbulence causing noticeable fluctuations in sensible heat flux. On rainy days, the dense cloud cover nearly eliminates solar radiation, resulting in lower ground

http://www.aloki.hu ● ISSN 1589 1623 (Print) ● ISSN1785 0037 (Online)
DOI: http://dx.doi.org/10.15666/aeer/2304_65756595

temperatures and reduced sensible heat fluxes. The daily cycle of sensible heat flux follows a gradient of clear days being the highest, cloudy days in the middle, and rainy days being the lowest, with peak values corresponding to this sequence.

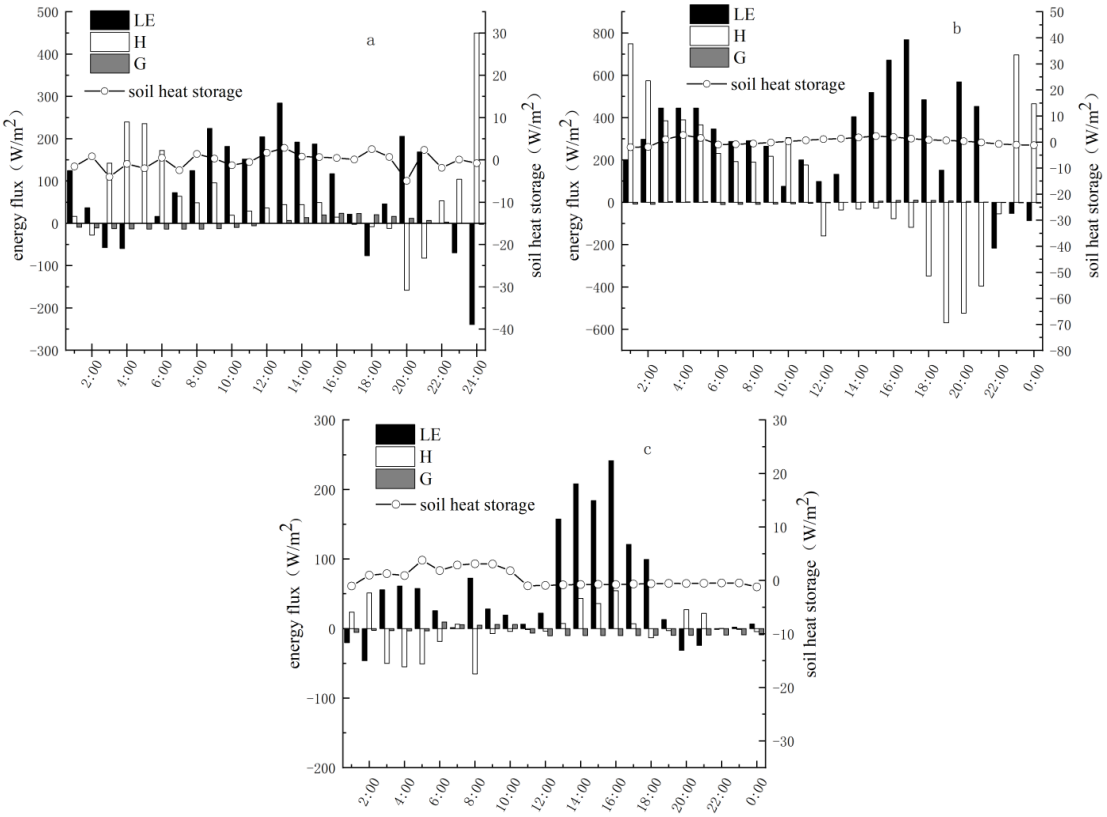

Figure 4. *On sunny (a), cloudy (b) and rainy (c) days, the energy changes of macrocystis ecosystem were observed*

In contrast to sensible and latent heat fluxes, soil heat flux assumes a relatively diminutive proportion, constituting 0.7%, -4.06%, and 0.47% of the net radiation on clear, cloudy, and rainy days, respectively. Soil heat flux experiences a pronounced decline on rainy and cloudy days, whereas it manifests a higher magnitude on clear days. The diurnal amplitude of soil heat flux, with clear days > cloudy days > rainy days, underscores the pivotal role of solar radiation and temperature in influencing soil heat flux dynamics.

In the context of soil thermal energy storage, positive values are observed on clear days, signifying the soil's absorption of energy. In contrast, on cloudy and rainy days, this metric takes on negative values, indicating an energy discharge from the soil into the atmosphere. Regardless of the prevailing weather conditions, the soil's thermal energy storage maintains a small and relatively stable absolute value.

All in all, weather conditions have significant effects on the dynamics of soil heat storage. On clear sky days, characterized by intense solar radiation and rising temperatures, the soil is in an energy absorption phase. On cloudy and rainy days, the heat storage trends of air and soil are parallel to each other, but there are obvious differences in the specific values and the stability of these indicators.

By averaging the energy under clear, cloudy, and rainy weather conditions, we obtain the changes in surface energy under average weather conditions. Comparing the energy

http://www.aloki.hu ● ISSN 1589 1623 (Print) ● ISSN1785 0037 (Online)
DOI: http://dx.doi.org/10.15666/aeer/2304_65756595

distribution under the three weather conditions with that under average weather conditions is shown in the *Table 2* below:

Table 2. *The change of parameters under different weather conditions*

	Annual data	Bare land				Giant Juncao land			
		Clear	Cloudy	Rainy	Average	Clear	Cloudy	Rainy	Average
Surface reflectance	0.280	0.289	0.282	0.248	0.273	0.308	0.309	0.317	0.311
LE/R_n(%)	81.83	70.42	74.30	64.03	71.97	74.01	70.63	71.53	72.61
H/R_n(%)	27.71	30.47	28.01	44.32	32.62	25.65	32.51	29.01	28.15
G/R_n(%)	-9.37	-0.38	-1.82	-7.16	-3.81	0.7	-4.06	0.47	-0.61

The table clearly illustrates that, across various weather conditions, the majority of surface energy is directed towards sensible and latent heat fluxes, with atmospheric energy being chiefly engaged in the exchange of heat and moisture. Relative to heat exchange with the atmosphere, the moisture exchange—specifically, the latent heat flux—between the Giant Juncao ecosystem and the atmosphere is notably more vigorous under average weather conditions. This heightened exchange is due to the robust structure of Giant Juncao, with its tall growth habit and a distinctive dual-phase bark and pith composition that facilitates swift water transport during solar-induced evaporation (Hu et al., 2014). Additionally, the Giant Juncao possesses an exceptionally low water evaporation enthalpy of 1.15 kJ/g, coupled with an extensive root system and physiological ecological traits, all of which enhance evaporation and atmospheric moisture exchange (Guo, 2023). The reduction in sensible heat flux over bare land on cloudy days, as opposed to clear days, is primarily linked to diminished solar radiation. Thicker cloud cover on cloudy days obstructs or disperses sunlight, resulting in reduced solar radiation at the surface and, consequently, less ground temperature increase compared to clear days, which in turn lessens the transfer of atmospheric heat. The pronounced moisture exchange and the greater allocation of energy to latent heat flux on cloudy days over bare land are attributed to the increased cloud cover and atmospheric turbulence, which promote more vigorous moisture exchange.

In the case of the Giant Juncao field, the soil heat flux is highest on clear days, followed by rainy days, and then cloudy days. This pattern is a consequence of the increased solar radiation on clear days, which elevates the overall energy and, subsequently, the soil heat flux. On cloudy days, the heightened atmospheric turbulence disrupts the stable energy exchange between the soil, vegetation, and atmosphere, leading to a transfer of some soil energy to the vegetation and atmosphere. In contrast, the energy dynamics over bare land on clear and cloudy days exhibit an inverse trend compared to the Giant Juncao field. Furthermore, under rainy conditions, the transfer of heat and moisture energy from the soil to the atmosphere is more pronounced over bare land. The soil heat flux under average weather conditions is comparatively higher for the Giant Juncao field, indicating a reduced release of energy, which underscores the protective influence of Giant Juncao on the energy dynamics of bare land. The presence of Giant Juncao is advantageous in mitigating the loss of soil heat flux, thereby fostering a more rational distribution of surface energy, particularly in semi-arid regions.

http://www.aloki.hu ● ISSN 1589 1623 (Print) ● ISSN1785 0037 (Online)
DOI: http://dx.doi.org/10.15666/aeer/2304_65756595

Change characteristics of evapotranspiration and Bowen ratio

Throughout the experimental period, the Bowen ratio and evapotranspiration (ET) exhibited significant variability, with the Bowen ratio ranging from -1 to 1, and ET fluctuating between -1.5 to 3.5 mm (*Figure 5*). These patterns align with previous studies on evapotranspiration in China's northwestern regions (Zhao et al., 2020). On clear days, the Bowen ratio and ET mirrored each other, both peaking initially and then declining. A sharp decline in the Bowen ratio was observed between 6:00 and 8:00, corresponding to a drop in ET between 16:00 and 18:00. Under clear skies, intense solar radiation and high surface temperatures significantly enhance the heat exchange between the ground and the atmosphere. During the early morning hours, increased surface humidity boosts evaporation, leading to a surge in latent heat flux and a rapid increase in ET rates. At this time, the Bowen ratio may decrease as the latent heat flux becomes more dominant over the sensible heat flux, highlighting a more pronounced evaporative cooling effect. As solar radiation strengthens on clear days, atmospheric heat exchange intensifies, with the Bowen ratio stabilizing and showing a downward trend. At night, around 20:00, the surface cools due to diminishing solar radiation, while the atmospheric layer, having absorbed heat during the day, cools more slowly, creating a significant temperature gradient between the surface and the atmosphere. This results in heat exchange primarily as sensible heat flux. ET on clear days initially increases and then decreases, tracking the sun's path and the strengthening of solar radiation. Solar radiation acts as the catalyst for ET, initiating the evaporation of surface moisture. Additionally, the gradual rise in temperature accelerates the evaporation process. Moderate wind speeds can also carry away moisture near the surface, further promoting evaporation. These factors collectively drive an upward trend in ET during the day. However, as the day progresses, solar radiation weakens, and temperatures drop. The interplay of these factors leads to a gradual reduction in the rate of evaporation. Especially after sunset, when the surface loses its solar energy source, the rate of evaporation declines further. Moreover, as the surface cools overnight and the temperature difference with the atmosphere increases, this may lead to the formation of an inversion layer near the surface, hindering the diffusion of water vapor and further reducing ET. At 18:00, a significant decrease in ET is observed, a time when solar radiation has waned, atmospheric temperatures have dropped, and the surface, warmed by the day's accumulated solar energy, remains relatively warm, with energy at this time primarily exchanged as heat.

Under overcast conditions, the Bowen ratio and evapotranspiration (ET) exhibit distinct diurnal patterns. The Bowen ratio varies between -0.4 and 0.2, while ET ranges from -0.1 to 0.4. The nocturnal changes in the Bowen ratio are significant, closely associated with temperature dynamics, wind velocity, and the saturation vapor pressure deficit. During daylight hours, the Bowen ratio initially increases and then declines. On cloudy days, despite reduced solar irradiance, the summer's thermal increase promotes atmospheric heat exchange, with the sensible heat flux rising in line with ambient temperatures. Around 13:00 under overcast skies, the Bowen ratio peaks, indicating the height of sensible heat flux allocation and suggesting that atmospheric energy is primarily conducted as heat. Conversely, at midnight, the Bowen ratio reaches its lowest point, with moisture exchange dominating atmospheric interactions. The average Bowen ratio on overcast days is -0.11. In contrast, ET decreases at night due to reduced atmospheric heat and moisture exchange, a sharp contrast to the daytime increase driven by temperature-induced transpiration in vegetation. As the day progresses and atmospheric temperatures rise, heat stimulates the evaporation of moisture from vegetation. After 14:00, at the

http://www.aloki.hu ● ISSN 1589 1623 (Print) ● ISSN1785 0037 (Online)
DOI: http://dx.doi.org/10.15666/aeer/2304_65756595

thermal peak of the day, plant leaves close their stomata as an adaptive response to prevent excessive water loss, leading to a significant decrease in ET. By 18:00, as temperatures drop and stomata reopen, ET briefly revives, only to be moderated by the cooling temperatures that once again limit the process.

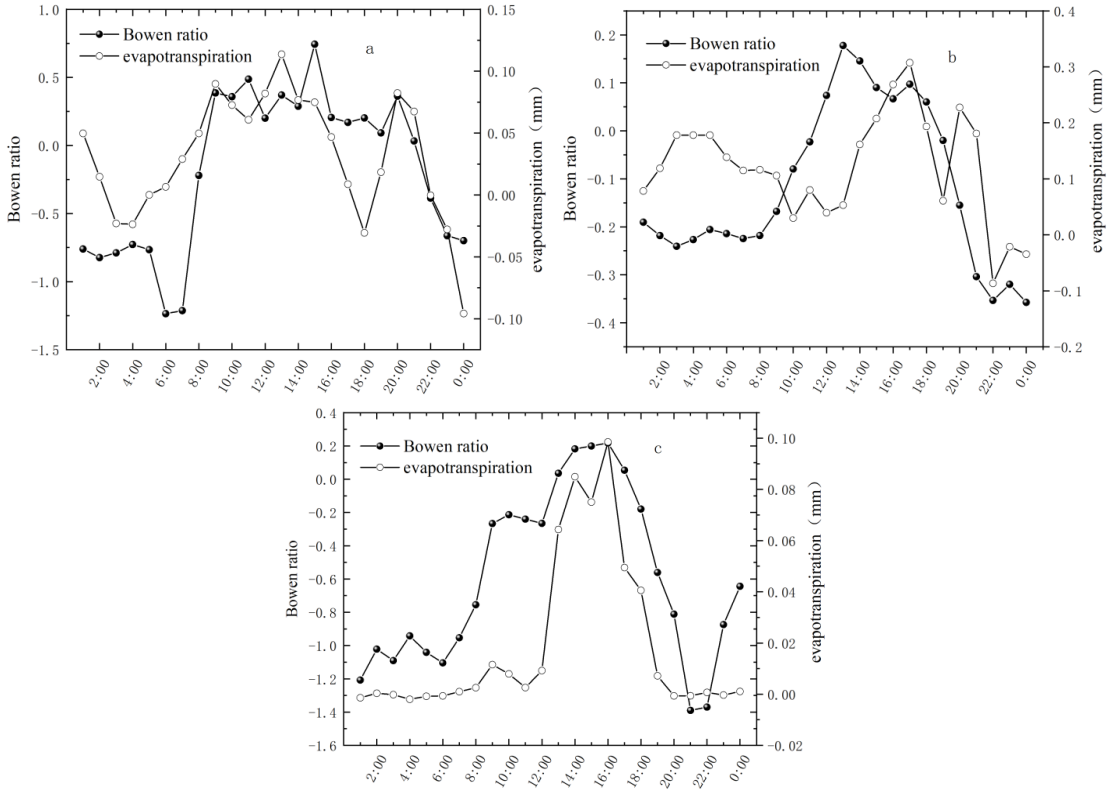

Figure 5. *Evapotranspiration and Berween ratio under sunny (a), cloudy (b), rainy (c) weather conditions*

The correlation between ET and meteorological factors under various weather conditions is shown in *Table 3* below. Under clear skies, the positive correlation between evapotranspiration (ET) and solar radiation is notably robust ($p < 0.01$), a correlation that can be traced back to the invigoration of solar radiation. This increase in solar intensity leads to a rise in surface temperatures, thereby catalyzing the process of evaporation. In tandem, the negative correlation between soil moisture and ET is equally statistically pronounced ($p < 0.01$), signifying that in arid soil conditions, plant transpiration is curtailed, while soil evaporation becomes relatively more pronounced.

Table 3. *Correlation between ET and various meteorological factors*

ET factors	Temperature	Soil moisture content	Solar radiation	Wind speed	Atmospheric humidity
clear	0.26	-0.517**	0.599**	-0.028	-0.274
cloudy	0.657**	-0.606**	0.943**	0.567**	-0.416**
rainy	-0.493**	-0.267	0.8**	0.57**	-0.387

Note: **. The correlation was significant at level 0.01

http://www.aloki.hu ● ISSN 1589 1623 (Print) ● ISSN1785 0037 (Online)
DOI: http://dx.doi.org/10.15666/aeer/2304_65756595

Dominant factors of evapotranspiration and energy distribution under different weather conditions

ET dominant factor analysis

The correlation between ET and meteorological factors under various weather conditions is shown in *Table 3*. Under clear skies, the positive correlation between evapotranspiration (ET) and solar radiation is notably robust ($p < 0.01$), a correlation that can be traced back to the invigoration of solar radiation. This increase in solar intensity leads to a rise in surface temperatures, thereby catalyzing the process of evaporation. In tandem, the negative correlation between soil moisture and ET is equally statistically pronounced ($p < 0.01$), signifying that in arid soil conditions, plant transpiration is curtailed, while soil evaporation becomes relatively more pronounced.

On rainy days, despite generally low levels of solar radiation, brief increases during lulls in rainfall can rapidly boost evapotranspiration (ET). An increase in wind velocity aids in the dispersal of water vapor, thereby enhancing the evaporation of moisture from vegetation, including species such as Giant Juncao. Under overcast conditions, ET shows a strong correlation with various meteorological factors ($p < 0.01$), with the relationship between solar radiation and ET being notably pronounced. This emphasizes the critical role of solar radiation as the primary driver of ET. At the same time, the negative correlation between atmospheric humidity and ET is less pronounced, suggesting that higher atmospheric humidity somewhat inhibits the evaporation of plant moisture.

A holistic assessment of the determinants of ET across varying weather scenarios underscores the pivotal influence of solar radiation on ET. This conclusion aligns with the research outcomes of scholars like Monteith and Jackson, further substantiating the significance of solar radiation as a key driver of evapotranspiration (Xiao et al., 2011; Tan et al., 2024).

Dominant factor analysis of energy distribution

The correlation between energy distribution and meteorological factors under varying weather conditions is detailed in *Table 4*. Under clear skies, the partitioning of surface energy is predominantly influenced by meteorological elements such as air temperature, solar radiation, and atmospheric humidity. Both air temperature and solar radiation exhibit a positive correlation with the Bowen ratio, signifying that a rise in temperature and an increase in solar radiation tend to augment the sensible heat flux relative to the latent heat flux (Robinson, 2009; Jobson, 1982). This trend can be ascribed to the escalation of sensible heat flux due to elevated temperatures and the heightened conversion of absorbed solar radiation into sensible heat when solar radiation intensifies. Conversely, atmospheric humidity is negatively correlated with the Bowen ratio, implying that in conditions of high humidity, the augmentation of evaporation and transpiration leads to an increase in latent heat flux, which in turn diminishes the Bowen ratio (Robinson, 2009). On cloudy days, the surface energy distribution is influenced by multiple meteorological factors, yet solar radiation remains the most influential, with its fluctuations directly impacting the partitioning of sensible and latent heat (Bowen, 1926). During rainy days, even transient increases in solar radiation can markedly affect the distribution of surface energy, while an uptick in wind speed aids in the dissipation of sensible heat and fosters the evaporation of moisture from the surface of vegetation, thus enhancing latent heat flux (Lian et al., 2010). Consequently, wind speed is highly

http://www.aloki.hu ● ISSN 1589 1623 (Print) ● ISSN1785 0037 (Online)
DOI: http://dx.doi.org/10.15666/aeer/2304_65756595

correlated with energy distribution, underscoring its pivotal role in modulating the surface energy balance.

Table 4. *Correlation between Bowen ratio and various meteorological factors*

Bowen ratio factors	Temperature	Soil moisture content	Solar radiation	Wind speed	Atmospheric humidity
clear	0.78**	-0.222	0.828**	-0.116	-0.776**
cloudy	0.726**	-0.432**	0.85**	0.676**	-0.499*
rainy	-0.613**	-0.241	0.898**	0.786**	-0.165

Note: **. The correlation was significant at level 0.01

Solar radiation and air temperature are key drivers in the distribution of energy across various weather conditions. On cloudy and rainy days, wind velocity plays a crucial role in energy partitioning, particularly in the realm of latent heat flux. This is achieved by dispersing sensible heat throughout the atmosphere and by accelerating the evaporation of moisture from plant surfaces. Under clear skies, however, an increase in atmospheric humidity leads to a decrease in the Bowen ratio. This decrease signifies an increased share of latent heat flux, while the proportion of sensible heat flux correspondingly decreases.

Evapotranspiration and energy distribution control factors

Combined with the above analysis of the leading factors of ET and Bowen ratio, the leading factors affecting ET and Bowen ratio can be obtained as follows (*Table 5*):

Table 5. *Correlation analysis between ET and Bowen ratio control factors*

Weather conditions	ET dominant factor	Bowen ratio dominant factor
clear	solar radiation+、soil moisture content-	temperature+、solar radiation+、atmospheric humidity-
cloudy	temperature+、solar radiation+、soil moisture content-	solar radiation+、wind speed+、temperature+
rainy	solar radiation+	solar radiation+、wind speed+、temperature-

Note: "+" and "-" represent positive correlation and negative correlation respectively

Key meteorological factors that significantly influence evapotranspiration (ET) encompass solar radiation, air temperature, soil moisture content, and wind velocity. During overcast and clear conditions, a marked negative correlation is observed between soil moisture content and ET, whereas solar radiation exhibits a positive correlation with ET. Conversely, under rainy conditions, the correlation between solar radiation and ET inverts to negative, while air temperature maintains a positive association with ET irrespective of the weather. The determinants of the Bowen ratio align positively with solar radiation, wind speed, and air temperature under clear skies, yet under rainy conditions, they inversely relate to solar radiation and wind speed. These findings underscore the variability of the predominant meteorological factors that sway ET and the Bowen ratio across different weather scenarios, with their fluctuations being subject

http://www.aloki.hu ● ISSN 1589 1623 (Print) ● ISSN1785 0037 (Online)
DOI: http://dx.doi.org/10.15666/aeer/2304_65756595

to a spectrum of meteorological influences. This research establishes a foundational premise for future investigations into the intricate mechanisms through which meteorological factors modulate evapotranspiration and the Bowen ratio.

Discussion and conclusion

Discussion

The influence of diverse weather conditions on ecosystem energy balance is notably significant. In China, comprehensive studies have been undertaken to examine the radiation and surface energy balance across a spectrum of weather conditions in various ecosystems. In the Gurbantunggut Desert, energy patterns display a unimodal shift on clear days and a concave variation on cloudy days (Li and Hu, 2021). Within the Badain Jaran Desert's interior during non-rainy weather, the energy interchange between the land and the atmosphere is primarily sensible heat, with a minor latent heat component, and the soil heat flux constitutes merely about 15% of the net radiation (Ma et al., 2015). On the northern slopes of the Tianshan Mountains, within the oasis-desert transition zone, the grassland's energy flux curves trace a unimodal shape on clear days, a polymodal pattern with frequent peaks and valleys on cloudy days, and a biased peak on rainy days, with energy transfer predominantly steered by latent heat, succeeded by sensible heat and soil heat flux (Yan et al., 2015). By the Eling Lake at the source of the Yellow River, the daily integrated values of sensible and soil heat fluxes exceed those on cloudy or rainy days, whereas the daily integrated value of latent heat flux is less than on cloudy or rainy days (Tang et al., 2013). In the desert riverbank's willow shrub communities, the daily fluctuation curves of the energy balance components are unimodal on clear days, with bimodal or multimodal patterns prevailing on cloudy, rainy, and dusty days (Ma et al., 2014).

These findings from arid and semi-arid areas, including desert interiors, desert transition zones, lakeside meadows, and riverbanks, align with the conclusions of this paper. Clear days are predominantly characterized by heat exchange, while cloudy and rainy days bring unstable energy shifts, a notable rise in latent heat flux, and more pronounced fluctuations. Notably, the average surface albedo of the grassland by the Eling Lake of the Yellow River source is 0.21, lower than the Giant Juncao field's albedo of 0.28, and the Xilin Hot grassland's albedo of 0.29 (Robinson, 2009), which is slightly higher than that of the Giant Juncao ecosystem. However, as the observation periods do not perfectly align, this comparison serves as a reference and does not conclusively demonstrate that the Giant Juncao ecosystem's surface albedo is lower than the Xilin Hot grassland's and higher than the grassland by the Eling Lake of the Yellow River source.

In conclusion, the surface energy distribution within the Giant Juncao ecosystem mirrors that of most arid and semi-arid ecosystems. This study investigated the changes of energy and radiation in the Giant Juncao ecosystem in the semi-arid region under different weather conditions, which is of great importance to deepen our understanding of the water budget, land use and inherent energy cycle of the Giant Juncao ecosystem in the semi-arid region. It is helpful to provide technical support and scientific guidance for providing reasonable irrigation management measures for the subsequent promotion of Giant Juncao in semi-arid areas and equatorial regions.

http://www.aloki.hu ● ISSN 1589 1623 (Print) ● ISSN1785 0037 (Online)
DOI: http://dx.doi.org/10.15666/aeer/2304_65756595

Conclusion

This study leverages data collected from July 1 to August 30 during the summer experimental period to analyze the radiation, energy, Bowen ratio, and evapotranspiration (ET) within the Giant Juncao ecosystem under clear, cloudy, and rainy conditions, reaching the following conclusions:

(1) On clear days, the Giant Juncao field experiences a unimodal change in solar radiation, surface reflected radiation, and net radiation, all peaking in the order of clear days > cloudy days > rainy days. Net radiation on cloudy days is highly variable, and on rainy days, it trends oppositely to solar and reflected radiation. Solar radiation peaks on clear days, with rainy days exceeding cloudy days. Reflected radiation is most pronounced on rainy days, surpassing that of clear and cloudy days. The diurnal range of net radiation is most extensive on clear days, followed by cloudy and rainy days.

(2) The surface albedo of the Giant Juncao field differs across weather conditions, with higher values in summer than the annual average. On clear days, albedo is lower compared to cloudy and rainy days. The cultivation of Giant Juncao, coupled with increased precipitation, significantly enhances surface albedo.

(3) Latent heat flux on clear days follows a unimodal pattern, a wavy trend on cloudy days, and on rainy days, its magnitude correlates with rainfall timing. Latent heat flux is diminished during rainfall, while it rises in the atmosphere outside of rainfall periods. Sensible heat flux under all conditions exhibits a unimodal change, with the most significant fluctuations on cloudy days. The diurnal range of sensible heat flux is most pronounced on clear days, followed by cloudy and rainy days. Similarly, the diurnal range of soil heat flux is greatest on clear days, then cloudy and rainy days. Soil thermal energy storage is positive on clear days, indicating soil energy absorption, and negative on cloudy and rainy days, indicating energy release to the atmosphere. The presence of Giant Juncao facilitates a rational distribution of surface energy.

(4) Throughout the experimental period, the Bowen ratio oscillates between -1 and 1, with evapotranspiration ranging from -1.5 to 3.5 mm. The Bowen ratio and evapotranspiration under all weather conditions exhibit a unimodal change. Total evapotranspiration on clear days amounts to 0.74 mm, which is lower than on cloudy days (1.41 mm) and higher than on rainy days (0.45 mm). The average Bowen ratio is highest on cloudy days, followed by clear and rainy days, with sensible heat flux trending opposite to latent heat flux.

(5) Meteorological factors influencing evapotranspiration and the Bowen ratio vary by weather condition, with solar radiation as the predominant driver. Temperature, wind speed, and soil moisture content exhibit significant correlations with evapotranspiration and the Bowen ratio.

Declaration of competing interest. The authors declare that there is no conflict of interest.

Data availability. The data presented in this study are available on request from the corresponding authors.

Acknowledgements. This work was financially supported by the Fujian Province Natural resources Department project (KKY22003XA);National Forestry and Grassland Administration (NFGA) “Unveiling the List and Appointing the Leader” Projects (202401–17);Major Science and Technology Special Project of Xinjiang Uygur Autonomous Region(2024A03009-5);The Science and Technology Program Project of Naqu City, Tibet Autonomous Region(NQKJ-2024-20);Fujian Agriculture and Forestry University Special Fund for Scientific and Technological Innovation Projects(KFB23189A).

http://www.aloki.hu ● ISSN 1589 1623 (Print) ● ISSN1785 0037 (Online)
DOI: http://dx.doi.org/10.15666/aeer/2304_65756595

REFERENCES

[1] Bowen, I. S. (1926): The ratio of heat losses by conduction and by evaporation from any water surface. – Physical Review 27(06): 779-787.
[2] Guo, Y. H. (2023): Study on the influence of bidirectional reflection characteristics of maize canopy on soil moisture estimation by UAV multi-spectral remote sensing. – Type, Northwest A&F University. DOI:10.27409/d.cnki.gxbnu.2023.001216.
[3] Hu, J., Chen, W., Zhao, B., Song, H. (2014): Winter performance test of PV-ETFE air pillow system. – Journal of Zhejiang University (Engineering Edition) 48: 1816-1821.
[4] Hu, Y., Zhang, Q., Xiao, G., Qiu, Z., Li, Y. (2022): Effects of soil carbon, nitrogen and phosphorus contents on maize production in semi-arid areas of China. – China Desert 42: 261-273.
[5] Jackson, R. D., Reginato, R. J., Idso, S. B. (1977): Wheat canopy temperature: A practical tool for evaluating water requirements. – Water Resour Res 13: 651-656.
[6] Jobson, H. E. (1982): Evaporation into the Atmosphere: Theory, History, and Applications. – EOS, Transactions American Geophysical Union 63(51): 1223-1224.
[7] Li, J., Ao, Y., Li, Z. (2012): Comparative analysis of desert radiation and energy balance under different weather conditions in summer. – Progress in Geography 31: 1443-1451.
[8] Li, H., Zhang, Q., Wang, C., Yang, F., Zhao, J. (2012): Effects of air heat storage, photosynthesis and soil vertical water movement on surface energy balance in the Loess Plateau. – Acta Physica Sinica 61: 537-547.
[9] Li, L., Yan, R., Xiong, H. (2018): Land surface energy balance of oasis-desert ecotone and its relationship with surface temperature during the summer. – Applied Ecology and Environmental Research 16(05): 5447-5465.
[10] Li, R., Liang, H., Yao, Y., Liu, J., Fu, S., Guo, J., Lin, C. (2019): Bibliometric analysis of macrophyta research literature in China based on CNKI database. – Anhui Agricultural Science Bulletin 25: 159-161.
[11] Li, C., Hu, S. (2021): Diurnal variation of energy flux of *Haloxylon ammodendron* community in the southern margin of Gurban Tungut Desert under different weather conditions. – Journal of University of Chinese Academy of Sciences 38: 567-575.
[12] Li, Q., Liu, S., Gao, G., Zhang, X. (2022): Characteristics and simulation estimation of surface soil heat flux in Ejin Oasis. – Desert of China 42: 176-184.
[13] Lian, T., Ren, G., Rong, H. (2010): Variability of Surface Sensible Heat Flux over Northwest China. – Atmospheric and Oceanic Science Letters 3(2): 75-80.
[14] Lin, X., Lam, C., Lin, D., Lin, H., Luo, H., Hu, Y., Lin, C., Zhu, C. (2014): Effects of macrophyta planting on functional diversity of soil microbial community and soil fertility on barren slope. – Acta Ecologica Sinica 34: 4304-4312.
[15] Liu, B., Yang, X., Song, N. (2010): Development prospect and countermeasures of fungus technology industry in Ningxia. – Ecological Economy 26(01): 147-150.
[16] Liu, F., Lin, X., Lin, H., Luo, H., Su, D., Cai, Y., Lin, Z. (2018): Study on the influence mechanism of evapotranspiration of giant fungus. – Journal of Fujian Agriculture and Forestry University (Natural Science Edition) 47: 748-754.
[17] Liu, F., Ba, N., Lam, C., Lin, D., Wang, P., Su, D. (2023): Evapotranspiration process and influencing factors of megaloweed based on Bowen ratio system. – Journal of Fujian Agriculture and Forestry University (Natural Science Edition) 52: 258-264.
[18] Ma, H., Chen, Y., Li, W. H. (2014): Energy balance characteristics of *Tamarix chinensis* shrubbery on desert riverbanks. – Chinese Journal of Desert 34(01): 108-117.
[19] Ma, N., Wang, N., Huang, Y., Li, H., Lu, J. (2015): Comparison of land-surface radiation budget and energy distribution characteristics under different weather conditions in the hinterland of Badain Jaran Desert in summer. – Journal of Natural Resources 30: 796-809.
[20] Monteith, J. L. (1981): Evaporation and Surface Temperature. – Q J Roy Meteor Soc 107(451): 1-27.

http://www.aloki.hu ● ISSN 1589 1623 (Print) ● ISSN1785 0037 (Online)
DOI: http://dx.doi.org/10.15666/aeer/2304_65756595

[21] Nie, Z., Mai, T. A., Mai, T. I., Yang, F., Alekun, A., Qi, F., Liu, Y. (2019): Comparative study on estimation of surface soil heat flux under different weather conditions in the hinterland of Taklimakan Desert. – Chinese Journal of Soil Science 50: 1306-1314.
[22] Rathod, M. K., Banerjee, J. (2013): Thermal stability of phase change materials used in latent heat energy storage systems: A review. – Renewable and Sustainable Energy Reviews 18: 246-258.
[23] Robinson, P. J. (2009): Sellers, W.D. 1965: Physical climatology. Chicago: University of Chicago Press, 272 pp. – Progress in Physical Geography 33(1): 130-132.
[24] Sheng, L. (2023): Application of macrophyta in ecological management of Ulan Buhe Desert. – Inner Mongolia Forestry 5: 34-35.
[25] Smith, W. K., Dannenberg, M. P., Yan, D., Herrmann, S., Barnes, M. L., Barron-Gafford G. A., Biederman, J. A., Ferrenberg, S., Fox, A. M., Hudson, A., Knowles, J. F., MacBean, N., Moore, D. J. P., Nagler, P. L., Reed, S. C., Rutherford, W. A., Scott, R. L., Wang, X., Yang, J. L. (2019): Remote sensing of dryland ecosystem structure and function: Progress, challenges, and opportunities. – Remote Sensing of Environment 233: 111401.
[26] Song, S., Lin, D., Zhou, H., Luo, Z., Zhang, L., Yi, C., Lin, H., Lin, X., Liu, B., Su, D. W., Zheng, D., Yu, S. K. (2023): Effects of macrophyta planting on plant species diversity and soil physicochemical properties in Ulan Buhe Desert. – Journal of Ecology and Environment 32: 1595-1605.
[27] Tan, C. S., Wu, X. M., Xia, L. M., Su, J. Y., Wu, J. Y., Yu, Y., Yang, R. L. (2024): JUNCAO-Stem-Based Interfacial Solar-Driven Evaporator with Natural Two-Phase Composite Structures of Functional Partition and Inherent Ultralow Vaporization Enthalpy of Water for Stable and Efficient Steam Production. – ACS Applied Materials & Interfaces 16(3): 11.
[28] Tang, T., Wang, L., Wen, X. (2013): Study on characteristics of radiation budget and surface energy balance in the area of Eling Lake, the source of the Yellow River. – Glaciology and Geocryology 35: 1462-1473.
[29] Ullah, S., You, Q., Sachindra, D. A., Nowosad, M., Ullah, W., Bhatti, A. S., Jin, Z., Ali, A. (2022): Spatiotemporal changes in global aridity in terms of multiple aridity indices: An assessment based on the CRU data. – Atmospheric Research 268: 105998. DOI:10.1016/j.atmosres.2021.105998.
[30] Wang, H., Li, D. L. (2011): Correlation of surface sensible heat flux in the arid region of northwestern China with the northern boundary of the East Asian summer monsoon and Chinese summer precipitation. – Journal of Geophysical Research: Atmospheres 116(19). DOI:10.1029/2011JD015696.
[31] Wang, A., Shang, Z., Zhang, M., Wang, G., Hu, X., Xu, F., Sun, Z., Cao, S., Liu, W., Fan, J., Zhou, Y. (2024): Study on dynamic monitoring and disease estimation model of wheat Powdery Mildew spores in field air based on spore capture and real-time PCR. – Plant Protection 50: 49-56.
[32] Xia, Z., Wang, S., Yi, X., Wang, Y., Fang, W. (2023): Method of unattended field measurement of surface reflectivity. – Optical Precision Engineering 31: 2319-2332.
[33] Xiao, D., Tao, F., Moiwo, J. P. (2011): Research progress on surface albedo under global change. – Advances in Earth Sciences 26(11): 1217-1224.
[34] Xu, Z., Liu, S., Xu, T., Ding, C. (2013): Comparison of different soil heat flux measurement methods and study of their effects on the closure of land surface energy balance. – Advances in Earth Sciences 28: 875-889.
[35] Yan, R., Xiong, H., Chen, X. (2015): Study on surface energy flux of Achnatherum in oasis-desert transition zone at the northern foot of Tianshan Mountains. – Acta Ecologica Sinica 35: 1350-1358.
[36] Yang, Y. T., Roderick, M. L., Guo, H., Miralles, D. G., Zhang, L., Fatichi, S., Luo, X. Z., Zhang, Y. Q., McVicar, T. R., Tu, Z. Y., Keenan, T., Fisher, J. B., Gan, R., Zhang, X. Z., Piao, S. L., Zhang, B. Q., Yang, D. W. (2023): Evapotranspiration on a greening Earth. – Nature Reviews Earth & Environment 4(9): 626-641.

http://www.aloki.hu ● ISSN 1589 1623 (Print) ● ISSN1785 0037 (Online)
DOI: http://dx.doi.org/10.15666/aeer/2304_65756595

[37] Zhang, Z., Liu, L., Li, X. (2019): Evapotranspiration characteristics of sunflower fields under drip irrigation under film in arid region. – Chinese Journal of Eco-Agriculture 27: 1195-1204.
[38] Zhao, Z., Wang, H., Wang, C., Li, W., Chen, H., Deng, C. (2020): Changes in reference evapotranspiration over Northwest China from 1957 to 2018: Variation characteristics, cause analysis and relationships with atmospheric circulation. – Agricultural Water Management 231: 105958-105958.
[39] Zhou, L. T., Huang, R. (2010): An Assessment of the Quality of Surface Sensible Heat Flux Derived from Reanalysis Data through Comparison with Station Observations in Northwest China. – Adv Atmos Sci 27: 500-512.
[40] Zhou, L. T., Huang, R. (2014): Regional differences in surface sensible and latent heat fluxes in China. – Theoretical and Applied Climatology 116: 625-637.

http://www.aloki.hu ● ISSN 1589 1623 (Print) ● ISSN1785 0037 (Online)
DOI: http://dx.doi.org/10.15666/aeer/2304_65756595